**A Novel Evaporative Cooling System with a Polymer Hollow Fibre Spindle**

Xiangjie Chen[1,3], Yuehong Su[1], Devrim Aydin[4], Yate Ding[1], David Reay[2], Richard Law[2], Saffa Riffat[1]

[1]Department of Architecture and Built Environment, University of Nottingham, University Park, NG7 2JQ, Nottingham. United Kingdom

[2]David Reay & Associates, United Kingdom

[3]Department of Energy and Power Engineering, University of Shanghai for Science and Technology, Jungong Road No. 516, Shanghai, 200031, China

[4]Department of Mechanical Engineering, Eastern Mediterranean University, G. Magosa, TRNC Mersin 10, Turkey

Contact: Saffa Riffat; Email: saffa.riffat @nottingham.ac.uk

Xiangjie Chen; Email: xiangjie.chen@nottingham.ac.uk

**Abstract**: A novel evaporative cooling system, in which the hollow fibre module constitutes as the humidifier and evaporative cooler, is proposed. With the aim to avoid the flow channelling or shielding of adjacent fibres the fibres inside each bundle were made into a spindle shape to allow maximum contact between the air stream and the fibres. This novel hollow fibre integrated evaporative cooling system will provide a comfortable indoor environment for hot and dry area. Moreover, the water vapour can permeate through the hollow fibre effectively, and the liquid water droplets will be prevented from mixing with the processed air. Under various inlet air dry bulb temperatures (27◦C, 30◦C, 33◦C, 36◦C and 39◦C), and various inlet air relative humidity (23%, 32% and 40%), the cooling performances of the proposed novel evaporative cooling system were experimentally investigated. The variations of outlet air dry bulb temperature, wet bulb effectiveness, dew point effectiveness and cooling capacity with respect to different incoming air dry bulb temperature were studied. The effects of various incoming air Reynolds number on the heat and mass transfer coefficients, heat flux and mass flux across the polymer hollow fibre module were analysed. Experimentally derived non-dimensional heat and mass transfer correlations were compared with other correlations from literature. Due to the spindle shape of proposed hollow fibre module, the shielding with hollow fibre bundles could be avoided greatly, therefore the mass transfer performance of the proposed system demonstrated significant improvement compared with other devices reported in literature.

**Key words**: Polymer hollow fibre, evaporative cooling, heat transfer, mass transfer, experiment

**Nomenclature**

| | |
|---|---|
| $A$ | Heat transfer area ($m^2$) |
| $C_p$ | Specific heat (kJ/kg K) |
| d | Fiber diameter (m) |
| $h$ | Heat transfer coefficient ($W/m^2K$) |
| $h_v$ | Enthalpy of saturated water vapour (kJ/kg); |
| $k$ | Mass transfer coefficient (m/s) |
| $L$ | Characteristic length of hollow fibre bundle (m) |
| $m$ | Mass flow rate (kg/s) |
| n | Number of fibres inside the heat exchanger |
| N | Mass flux ($mg/m^2$ s) |
| Nu | Nusselt number |
| Pr | Prandtl number |
| $q$ | Heat flux ($W/m^2$) |

| | |
|---|---|
| Re | Reynolds number |
| $Sh$ | Sherwood number |
| Sc | Schmidt number |
| $T$ | Temperature (˚C) |
| $U$ | Overall heat transfer coefficient (W/m$^2$K) |
| $V$ | Volumetric flow rate of the incoming air, m$^3$/h; |
| $Q$ | Sensible cooling capacity (W) |

**Greek Letters/Subscripts**

| | |
|---|---|
| $a$ | Air |
| dew | Dew point |
| dry | Dry bulb |
| e | Evaporated water |
| $\varphi$ | Packing fraction of the module |
| ε | Effectiveness |
| H | Heat transfer |
| λ | Thermal conductivity (W/mK) |
| M | Mass transfer |
| ρ | Density of the fluid (kg/m$^3$) |
| $u$ | Incoming air velocity, m/s |
| $\nu$ | Dynamic viscosity of the fluid (kg/ms) |

$\omega$ Humidity ratio of the air (kg/kg)

wb wet bulb

## 1. Introduction

Global energy demand is soaring during past few decades due to the rapid worldwide economy development and urban sprawl. According to the research report produced by International Institute of Refrigeration, air conditioning system accounts for 45% of the total energy consumption for domestic and commercial buildings[1]. Overall, air-conditioning system takes up approximately 15% of the total energy consumption around the world[1]. In the Middle East, where the climatic condition is dry and humid, air conditioning system consumes as high as 70% of energy required for buildings and around 30% of the total energy[2]. With the impact of global warming, the demands of effective air-conditioning system which consumes less energy and provide higher cooling performance is massive.

The current widely-used vapour compression system plays dominant role in the market. However, vapour compression system has the disadvantages of intensive energy consumption and low performance in hot and humid climate. Moreover, the possible leakage of high GWP refrigerants will lead to the depletion of Ozone Layer, which further contributes to the global warming and other associated environmental and social changes. Hence, the development of more energy efficient and environmental benign cooling systems remains to be the research topics for scientific researches.

In the past few decades, evaporative cooling system arouses great attentions among the researchers due to the fact that it is more environmentally friendly (use of the water as working fluids), simple in structure configuration, and less consumption in primary energy. Direct evaporative cooling system works under the following principle: the incoming hot and humid air gets direct contact with the circulating water, causing the evaporation of the water and the air temperature will be reduced accordingly. Consequently, the evaporated water, in the form of vapour will be absorbed by the air, which leads to the humidity increase of the outlet air.

Recently, the research interests of this topic are focused on pad incorporated evaporative cooling system[3-6], desiccant based evaporative cooling system[7, 8], and dew point based evaporative cooling system[9-12]. Due to the large contact surface area, porous pad incorporated evaporative cooling systems have attracted more attentions. Wu et al.[13] presented a simplified mathematical model to describe the heat and moisture transfer between water and air in a direct evaporative cooler, with pad thickness of 125mm and 260mm, the cooling efficiency reached 58% and 90% respectively. Franco et al. [14] studied the influence of water and air flows on the performance of cellulose media. The results showed that with a thickness of 85mm, a plastic grid pad could offer a cooling efficiency of 65% at wind speed of 1.5m/s. However, since water is directly in contact with the incoming air in the closed system, there is the potential for microbial growth due to the supply of stagnant water. This may provide an opportunity for the spread of liquid phase-born bacterial diseases for occupants[15].

In order to solve this problem, a hollow fibre integrated evaporative cooling system has been proposed. Compared with porous pad media, hollow fibre materials provide several advantages as follows: 1) allow selective permeation of moisture: with pore sizes less than 0.1μm, hollow fibre material will allow the water vapour transfer but eliminate the bacteria and fungi penetration[16]; 2) provide large surface area per unit volume[17], which is favourable for enhanced heat and mass transfer. Detailed descriptions about hollow fiber materials and their applications are summarized in the literature[18]. According to Chen et al.[19], the overall heat transfer coefficients could reach 1675W/m$^2$K with a fibre diameter of 550μm. Kachhwaha and Preahhakar[20] analysed heat and mass transfer performance for a direct evaporative cooler using a thin plastic plate. The experimental testing results indicated that the outlet air temperatures were between 21◦C and 23◦C, at the inlet dry bulb temperature of 24.8-28.4◦C, the air humidity ratio of 2.3-5.8g/kg and air mass flow rate of 0.13, 0.2, 0.3 and 0.4g/s. Zhang[21] proposed the theoretical investigations on a rectangular cross-flow hollow fibre membrane module for air humidification. With 2600 fibres (fibre outside diameter 1.5mm) inside the module, the outlet air temperature could reach 21.5◦C when the inlet dry bulb temperature was 30◦C. Johnson et al.[15] studied the heat and mass transfer of a hollow fibre membrane evaporative cooling system. With a different range of fibre bundles (9, 19, 29 fibre bundles), the heat transfer area was in the range of

0.35m$^2$-1.13m$^2$, and around 0.4◦C temperature drop could be observed from the experiments. The above publications are mainly concentrated on the theoretical analysis on the polymer hollow fibre integrated evaporative cooling system. The available experimental results were limited to the variation of outlet air temperatures with respect to different air flow rates. In addition, as stated by Johnson et al.[15], due to the shielding from adjacent fibres, the heat and mass transfer performance will decrease when using a large number of fibres inside one module.

A summary of the recent experimental and modelling works on evaporative cooling system is presented in Table 1. Literature review indicates that the previous published papers were mainly concentrated on the theoretically modelling of evaporative cooling system. For the limited experimental investigations reported in the literature, the evaporative coolers were mainly made from porous paper materials. This paper presents a novel evaporative cooling system with a hollow fibre evaporative cooler. Instead of previously reported cross flow configurations[13, 15, 21], five fibre bundles (each contains 100 fibres) with the distance of 5cm were placed normal to the air stream, with detailed configuration shown in Figure 2. In order to avoid the flow channelling or shielding of adjacent fibres, the fibres inside each bundle were made into a spindle shape to allow maximum contact between the air stream and the fibre. As a subsequent work of previous research[22], this research work extends the previous experimental testing conditions to a wider range, with the incoming air temperature up to 39◦C and relative humidity up to 40%. The variations of outlet air dry bulb temperature, wet bulb effectiveness, dew point effectiveness and cooling capacity were studied by varying the incoming air dry bulb temperature from 27◦C to 39◦C and RH from 23% to 40%. The effects of various incoming air Reynolds number on the heat and mass transfer coefficients, heat flux and mass flux across the polymer hollow fibre module were analysed. Two sets of experimentally derived non-dimensional heat and mass transfer correlations were summarized, which could be favourable for the future design of polymer hollow fibre integrated evaporative cooling system.

## 2. Heat and mass transfer of hollow fibre evaporative cooling system

The 3D model of the hollow fiber module is shown in Figure 1 together with the temperature and humidity change profile. As illustrated in Figure 1, the incoming hot and humid air gets in contact with the porous hollow fiber module, inside which the water will be circulating around. As water evaporates through the hollow fibers, it will extract energy from the incoming air causing the temperature to drop. As reported by Johnson et al.[15], the resistance of fibe materials is very small, therefore it could be neglected. According to Rawangkul et al[5],

The sensible cooling capacity ($Q_{\blacksquare}$) supplied by the incoming air of such novel evaporative cooling system can be calculated by:

$$Q_{\blacksquare} = m_a C_{pa}(T_1 - T_2) = \frac{C_{pa}\ \rho_{\blacksquare} V(T_1 - T_2)}{3.6} \qquad \text{Eq.(1)}$$

Where, Q is the flow of transferred heat (W);

$m_a$ is the mass flow rate of the incoming air (kg/h);

$C_{pa}$ is the specific heat of air at constant pressure, kJ/(kg K);

$T_1$ is the dry bulb temperature of the incoming air (◦C);

$T_2$ is the dry bulb temperature of the outgoing air (◦C);

$\rho_{\blacksquare}$ is the density of the air, kg/m$^3$;

V is the volumetric flow rate of the incoming air, m$^3$/h;

The rate of watere evaporation is:

$$m_e = m_a(\omega_2 - \omega_1) \qquad \text{Eq.(2)}$$

Where $m_e$ is the flow of evaporated water(kg/h);

$m_a$ is the mass flow rate of the incoming air (kg/h);

$\omega_1$ is the humidity ratio of the incoming air;

$\omega_2$ is the humidity ratio of the outgoing air.

The rate of heat transfer (Q) and the rate of water evaporation ($m_e$) can be given as the product of heat transfer coefficient and the mean logarithmic difference in temperature ($\Delta$T), and the product of the mass transfer coefficient and the mean logarithmic difference in the water vapour density ($\Delta\rho_V$). These can be expressed in the following two equations:

$$Q = h_H A_s \, \Delta T = qA_s \qquad \text{Eq.(3)}$$

$$m_e = h_M A_s \Delta\rho_V = NA_s \qquad \text{Eq.(4)}$$

Where $h_H$ is the coefficient of heat transfer (W/m$^2$K);

$h_M$ is the coefficient of mass transfer (W/m$^2$K);

q is the heat flux (W/m$^2$);

N is the mass flux (mg/ m$^2$s);

$A_s$ is the total surface area of the polymer hollow fibre (m$^2$);

The mean logarithmic difference in temperature ($\Delta$T) and water vapour density ($\Delta\rho_V$) can be calculated using following equations:

$$\Delta T = \frac{(T_2 - T_1)}{\ln(\frac{T_2 - T_{wb}}{T_1 - T_{wb}})} \qquad \text{Eq.(5)}$$

$$\Delta\rho_V = \frac{(\rho_{V2} - \rho_{V1})}{\ln(\frac{\rho_{V1} - \rho_{wb}}{\rho_{V2} - \rho_{wb}})} \qquad \text{Eq.(6)}$$

Where $\rho_{V1}$ and $\rho_{V2}$ are the water vapour density on entering and leaving the hollow fibres (kg/m$^3$);

$\rho_{wb}$ is the saturated water vapour density at the wet bulb temperature (kg/m$^3$).

The heat and mass transfer coefficients could be calculated from:

$$h_H = \frac{Nu * k}{d_h} \qquad \text{Eq.(7)}$$

$$h_M = \frac{Sh * D_{AB}}{d_h} \qquad \text{Eq.(8)}$$

Where k is the thermal conductivity of the air (W/mK);

$d_h$ is the hydraulic diameter of the hollow fibre module, m. According to [23], $d_h$ can be calculated as :

$$d_h = \frac{4\ cross\ sectional\ area\ of\ flow}{wetted\ perimeter} \qquad \text{Eq. (9)}$$

According to the hollow fiber bundle configuration[24], $d_h$ can further be expressed as:

$$d_h = \frac{4\ A_{flow}}{n\pi d_0 + \pi D} = \frac{(1-\varphi)D^2}{\pi d_0 + D} \qquad \text{Eq. (10)}$$

Where $\varphi$ is the packing fraction of the module;

$d_0$ is the outer diameter of a single fiber;

$D$ is the diameter of the module shell (m);

The relationship between Reynolds number (Re), Prandtl number (Pr) and Nusselt number (Nu), and the relationship between Reynolds number (Re), Schmidt number (Sc )and Sherwood number (Sh) can be expressed by:

$$Nu = C_1 Re^{m1} Pr^{1/3} \qquad \text{Eq.(11)}$$

$$Sh = C_2 Re^{m2} Sc^{1/3} \qquad \text{Eq.(12)}$$

Where $C_1$, $C_2$, $m_1$, $m_2$ are constants for the hollow fibre bundles.

Reynolds number can be calculated by:

$$\mathrm{Re} = \frac{u * d_h}{\nu} \qquad \text{Eq.(13)}$$

Where $u$ is the incoming air velocity, m/s;

$\nu$ is the viscosity of the incoming air, $m^2/s$.

From the previous study [22], using the experimental data, general empirical correlations for the non-dimensional heat and mass transfer data for the proposed system are derived using mathematical data regression techniques. In this research, as the experimental testing conditions are extended to a large range, the applicability of these equations will be verified in section 4.

$$Sh = 1.275 Re^{1/3} Sc^{1/3} \qquad \text{Eq. (14)[22]}$$

$$Nu = 0.958 Re^{1/3} Pr^{1/3} \qquad \text{Eq. (15)[22]}$$

The wet bulb effectiveness ($\varepsilon_{wb}$) is an important expression used to characterise the air saturation capacity of the polymer hollow fibre bundle. This is defined as the ratio between the thermal difference on passing through the hollow fibre bundle ($T_1 - T_2$) and the maximum thermal difference that would occur if the air were saturated ($T_1 - T_{wb}$):

$$\varepsilon_{wb} = \frac{T_1 - T_2}{T_1 - T_{wb}} \qquad \text{Eq.(16)}$$

Similarly, the dew point effectiveness ($\varepsilon_{dew}$) is defined as the ratio between the incoming air and the outgoing air to the difference between the incoming air and its dew point temperature, as indicated by the following expression:

$$\varepsilon_{dew} = \frac{T_1 - T_2}{T_1 - T_{dew}} \qquad \text{Eq.(17)}$$

## 3. Experimental testing rig

A lab scale experimental testing rig is developed, which integrates the hollow fiber evaporative cooler with the evaporative cooling system. Polyvinylidene fluoride (PVDF) hollow fibres (manufactured by ZENA Ltd.) with outside diameter of 0.8mm and inside diameter of 0.6mm, an effective pore size of 0.5µm and a porosity of 50% were used for the fabrication of the polymer hollow fibre module. The polymer hollow fibre module consists of 5 fibre bundles (each contains 100 fibres), which were connected at each bundle ends using T piece plastic tubing. The hollow fibre module was incorporated into a circular aluminium tunnel, whose cross section diameter was 0.15m. In order to avoid the flow channelling or shielding of adjacent fibres, the fibres in each bundle were compressed from both ends to make the bundle into a spindle shape to allow maximum contact between the air stream and the fibres. The detailed physical properties of the polymer hollow fibre module were summarized in Table 2.

The testing rig consists of a polymer hollow fibre module, an air tunnel, a water pump, a fan and a water tank. The detailed schematic diagram is shown in Figure 2. A 5-litre water tank was used to provide water circulation inside the fibre. In order to avoid any particle blockage within the polymer hollow fibres, a water filter was allocated to improve the purity of the incoming water into the fibres. A flow meter and a ball valve were included in the water circulation cycle with the aim to control the water flow rate inside the fibre. In order to minimize the experimental testing errors, four humidity and temperature sensors (EK-H4, Sensirion, UK) were located at the inlet (point 1 in Figure 2) and outlet (point 2 in Figure 2) of the tunnel respectively, to measure the inlet and outlet conditions of the air stream. Additional K type thermocouples were used to measure the water temperature entering and leaving the hollow fibre module (point 3 and 4 in Figure 2). The aluminium tunnel was connected with a variable frequency drive centrifugal fan, which was linked directly with the environmental chamber. The experimental prototype image is shown in Figure 3. The basic working principle of the experiment is as following: The hot and humid air from the environmental chamber will be blown out by the blower into the air tunnel. With the help of the circulation pump, water is circulating from the water tank into the hollow fibre bundles to ensure that the fiber surface will get wetted throughout the tests. The incoming hot and humid air will get in contact with the hollow fibre module. As water evaporates through the porous hollow fibres, the temperature of incoming air will be reduced, accompanied by the increased relative humidity.

At the beginning of each test, the environmental chamber was set to the required temperature and humidity level. As soon as the temperature and humidity reached the desired values, the water pump for the fibre module and the fan in the air stream direction was switched on. The air velocity was measured at the five different positions along the cross sections of the outlet aluminium tunnel, using the air velocity probes connected to a recorder (Testo 454). The dynamic pressures in the upstream and downstream of the air flow were recorded using Pressure transducers (Ge UNIK 5000).

For each test, the temperature and humidity values were recorded every 20 seconds until the time when the system reach steady states as indicated by the humidity and temperature sensor readings. The accuracy of the measuring instruments used was: ±0.2% for temperature, ±0.5% for pressure, ±2% for air velocity, and ±2% for relative humidity.

## 4. Results and discussion

As indicated in Table 3, the experiments were carried out for the proposed novel evaporative cooling system with various inlet air dry bulb temperatures (27◦C, 30◦C, 33◦C, 36◦C and 39◦C), and various inlet air relative humidity (23%, 32% and 40%). Figure 4 presents the variation of outlet air dry bulb temperatures with respect to various inlet air dry bulb temperatures under different incoming air relative humidity. For incoming air temperature in the range of 27-39◦C and the incoming air relative humidity varying from 23%, 32% to 40%, it can be observed that the outlet air temperature is dramatically affected by inlet air relative humidity at constant incoming air temperature. At the same inlet air dry bulb temperature, the higher incoming air relative humidity will lead to the lower outlet air dry bulb temperature. For instance, at the inlet air dry bulb temperature of 30◦C, the outlet air dry bulb temperature were 24.8◦C, 25.7◦C and 26.4◦C respectively for RH of 23%, 32% and 40%. This shows that the proposed novel evaporative cooling system has great potential to be used in hot and dry climatic conditions. On the other hand, Figure 4 shows that the outlet air dry bulb temperature tends to form a linear relationship with the inlet air dry bulb temperature at the same inlet air relative humidity. The slopes of the outlet air dry bulb temperature at constant relative humidity are in the range of 0.7-0.74. This means that, when increasing the inlet air temperature by 10◦C, the outlet air temperature will be improved by 7-7.4◦C.

Figure 4 also compares the proposed experimental testing data with the outlet dry bulb temperature presented by Dohnal, et al [25], for a compact bundle of 600 polyoropylene hollow fibres placed horizontally down the air stream, with the inlet air dry bulb temperature of 24.6◦C, and the RH= 25%. It can be found that the presented experimental results agrees well and even shows better cooling performance compared with the testing results obtained by Dohnal et al [25]. This might be due to the fact that the proposed evaporative cooling system adopted the novelty of using spindle shape fibre bundles to allow maximum contact between the air stream and the fibre. While in the experiments proposed by Dohnal et al. [25], the shielding from adjacent fibre in the entire bundles resulted in decreased heat transfer performance.

The wet bulb effectiveness of the proposed novel evaporative cooling system is illustrated in Figure 5. It can be found that, with the incoming air dry bulb temperature in the range of 27-39◦C, and RH of 23%, 32% and 40%, the wet bulb effectiveness varies from 0.32-0.45. Higher inlet air dry bulb temperature leads to greater wet bulb effectiveness, due to the fact that larger temperature depression is obtained for higher inlet air temperature. In addition, lower inlet air relative humidity will result in higher wet bulb effectiveness. The reason is due to the fact that drier incoming air with small relative humidity actually represents larger driving force of vapour pressure difference between the inlet and outlet air condition. Thus the direr incoming air can potentially absorb more moisture during the water evaporation process. Therefore, more latent heat will be required during the water evaporation process. Consequentially, a larger amount of sensible heat of the processed air will be transferred from the incoming dry air to the outgoing wet air. This leads to a much lower outlet air temperature compared with air of higher incoming relative humidity. Comparable value of wet bulb effectiveness obtained by Dohnal et al. [25] is also included in Figure 5. With the inlet air dry bulb temperature of 24.6◦C, and the RH= 25%, the wet bulb effectiveness achieved by Dohnal, et al. [25] was 0.354, which showed a good agreement with the presented experimental results.

Figure 6 illustrates the variations of dew point effectiveness with respect to different inlet air conditions. When air inlet dry bulb temperature increases from 27◦C to 39◦C, the dew point effectiveness is in the range of 0.18-0.3. At the same inlet air RH, higher inlet air temperature leads to higher dew point effectiveness, due to the fact that larger temperature depression is obtained for higher inlet air temperature. Moreover, when the inlet air dry bulb temperature maintains at the same level, lower inlet RH will result in higher dew point effectiveness. The reason is similar to what we present in last paragraph, as drier incoming air with smaller relative humidity actually represents larger driving force of vapour pressure, thus leads to higher cooling performance. The dew point effectiveness obtained in this experimental study is slightly better than the results achieved by Dohnal et al. [25], due to the fact that the at lower air velocity, the individual fibres within the bundles were shielded from the air stream, as the majority of the air will go past the outer layer of the fibre bundles. Therefore, such intra-bundle shielding effect in Dohnal et al. [25]'s testing configurations might lead to reduced heat transfer performance.

Figure 7 depicts the variations of cooling capacity with respect to various inlet air dry bulb temperatures under different incoming air relative humidity. Generally, the cooling capacity increases with the improvement of the inlet air dry bulb temperature from 27◦C to 39◦C. With the same inlet air dry bulb temperature, lower inlet air RH will lead to higher cooling capacity. For instance, when inlet air dry bulb temperature is fixed at 30◦C, the cooling capacities are 125.2W, 109.9W and 83.1W respectively for the inlet air RH equals to 23%, 32% and 40%. The reason is due to the fact that, as shown in Eq. (1), the cooling capacity is proportional related to the differences between the inlet air and outlet air dry bulb temperature. Drier incoming air with small relative humidity actually represents larger driving force of vapour pressure difference between the inlet and outlet air condition. Thus the drier incoming air can potentially absorb more moisture, which leads to a much lower outlet air temperature compared with air of higher incoming relative humidity. Therefore, the cooling capacity shows decreased trend when increasing the inlet air RH from 23% to 32% and 40%.

Figure 8 shows the experimental obtained heat flux under different incoming air relative humidity. It can be observed that the heat flux will increase with the improvement of incoming air Reynolds number. At the same Reynolds number, lower inlet air relative humidity will lead to greater heat flux. For instance, at Reynolds number of 100, the heat flux increases from 798W to 1512W respectively for RH equals to 40% and 23%. This means that approximately 1.8 times more heat is transferred in the process when RH decreased from 40% to 23%. The reason is because, as shown in Eq. (3), the heat flux is positively related to the inlet and outlet air dry bulb temperature difference. Moreover, as shown in Figure 5, lower inlet air relative humidity will yield much lower outlet air dry bulb temperature, which means greater inlet and outlet air dry bulb temperature difference. This will consequentially lead to higher heat flux. Similar trend could be found in Figure 9, showing the variations of mass flux with respect to Reynolds number under different incoming air RH. It is obvious that higher Reynolds number will contribute to greater mass flux under the same RH. While for the same Reynolds number, lower RH will lead to higher mass flux.

Experimental determined overall heat transfer coefficient ($h_H$) and mass transfer coefficients ($h_M$) with respect to Reynolds number under different inlet air relative humidity are illustrated in Figure 10 and Figure 11. An increase in Reynolds number yields better heat and mass transfer between the air stream and the water inside polymer hollow fibre. Despite of different inlet air relative humidity, $h_H$ follows the same linear relationship with Reynolds number, with variations less than 4.1% during the experiments. The similar linear relationship between Reynolds number and $h_M$ is illustrated in Figure 11. Further inspection of Figure 10 and Figure 11 indicate that, by increasing Reynolds number from 0 to 220, $h_H$ changes from around 60 W/m$^2$K to 250 W/m$^2$K (about 4.2 times), while $h_M$ improves from 0.01m/s to 0. 25m/s respectively (about 2.5 times). This indicates the changes of Reynolds number has more significant impact on the heat transfer coefficients than the mass transfer coefficients for the proposed polymer hollow fibre integrated evaporative cooling system.

Figure 12 and Figure 13 respectively illustrated the non-dimensional heat and mass transfer data. It is evident that the three different testing conditions yield more or less the same linear relationship between the logarithm value of Sh/Sc$^{1/3}$, Nu/Pr$^{1/3}$ and logarithm value of Reynolds number.

The heat and mass transfer data are correlated by an empirical equation as shown in Eq. (11)-(12). The Reynolds number exponent, α, in the Eq. (11)-(12) is an indication of the flow conditions. For example, α=1/3 indicates laminar flow with fully developed velocity profile. According to literature[26], for α=0.5, the indication is for developing velocity and concentration profiles, which is in the entry region condition[27]. For α approaching 0.8-1.0, the flow is in the turbulent flow regime. For the proposed novel evaporative cooling integrated hollow fibre system, the low Reynolds number (less than 300) clearly shows the laminar flow regime. Therefore, the exponent α, for this study will be chosen as 1/3.

After obtaining the heat and mass transfer coefficients $h_H$ and $h_M$, based on Eq. (7) and Eq. (8), Nu and Sh number can be calculated accordingly. Reynolds number can be obtained by inserting experimental measured air velocity and hydraulic diameter of the hollow fiber module into Eq. (13). Pr number of  is taken as 0.713 under the air temperature of 20°C. Based on the experimental obtained data, general empirical correlations for the non-dimensional heat and mass transfer data of the proposed system are derived using mathematical data regression techniques:

$$Sh = 1.134Re^{1/3}Sc^{1/3} \quad \text{Eq. (18)}$$

$$Nu = 0.976Re^{1/3}Pr^{1/3} \quad \text{Eq. (19)}$$

The above experimental determined correlation for the non-dimensional heat and mass transfer data of the polymer hollow fibre integrated evaporative cooling system are compared with the results (Eq. (20) and Eq. (14)- (15) obtained by Yang and Cussler[28] and X. Chen et al.[22]. Data from Yang and Cussler[28] and X. Chen et al.[22]'s experiments showed that the exponent of Reynolds number were both equal to 1/3, while the constant for heat transfer correlations were 1.38 and 1.275 respectively. The deviation of the constants for Eq. (18) and Eq.(20) is 21.7%. This is due to the fact  that Yang and Cussler[28]'s experimental testing rig contained 750 fibers (outside diameter 0.4mm) inside the module for a liquid-gas heat and mass transfer process, while in the proposed system the fiber number is reduced to 500 with larger outside diameter of 0.8mm. Such difference in testing configurations could lead to the discrepancy between the two constants in the equations. On the other hand, different from the subsequent work of previous research[22], the present work offers a wider range of testing conditions, for inlet air temperature and relative humidity up to 39◦C and 40%. However, the deviations of the two heat transfer constants and mass transfer constants for the present research and the previous study are very small, with only 12.3% and 2.1%, as indicated in Eq. (18)-(19) and Eq. (14)-(15). Such deviations could be due to the unavoidable experimental errors. For instance, performing the uncertainty analysis proposed by Moffat[29] for Equation (13), the obtained uncertainty of the Reynolds number is 5.3%. Therefore, it can concluded that for a wider range of testing conditions, the obtained heat and mass transfer correlations actually agree well with the previous research[22]. This further proves that the testing conditions do not have significant effects on the non-dimensional heat and mass transfer data.

$$Sh = 1.38Re^{0.4}Sc^{1/3} \qquad \text{Eq. (20)[28]}$$

Experimental obtained mass transfer data in comparison with other correlations from literature is presented in Figure 14. Different groups of mass transfer correlations developed by Zhukauska[30], Yang and Cussler[28], Cote et al.[31], Chen et al.[22] and Johnson et al.[15] were used to perform the comparisons. The results obtained from the proposed novel evaporative cooling system is similar to Cote et al.[31]'s correlation, where the fibre bundle was used to transport oxygen through water. The presented results are also very close to Johnson et al.[15]'s correlation, which was obtained from the fibre array integrated evaporative cooler. It is also possible to observe that the mass transfer data for the present research agrees relatively well with those obtained from the previous research[22]. Furthermore, Figure 14 demonstrated that the mass transfer performance for the fibre bundles (29 fibres included) achieved by Johnson et al.[15] are the worst compared with other fibre configurations. In the present study, the fibre module consists of 5 fibre bundles which contain 100 fibres individually. However, the mass transfer performance of such proposed fibre module shows significantly improvement compared with the mass transfer conditions of fibre bundles presented by Johnson et al. [15]. The reason is due to the fact that, the spindle shape in the proposed system helps to avoid any over-shielding effect within the fibre bundle. By compressing the fibre from both ends, the loosed spindle shape fibre bundle could be obtained, which helps to enable better heat and mass transfer between each individual fibre and the incoming air. For normal shape fibre bundle, such shielding effect is more significant at lower Reynolds number, when the air will go past the outside of the fibre bundle, leaving the majority of the fibre inside the bundle with very little contact with the incoming air. As the Reynolds number increases, better contact between the fibres inside the bundle could be achieved, which leads to better mass transfer performance, as shown in Figure 14.

## 5. Conclusions

A novel evaporative cooling system with hollow fiber bundles in the spindle shapes is proposed in this research. With the aim to avoid the flow channelling or shielding of adjacent fibres, the fibres were compressed into a spindle shape to allow maximum contact between the incoming air and the fibres. This novel hollow fibre integrated evaporative cooling system will provide a comfortable indoor environment for hot and dry area. Under various inlet air dry bulb temperatures (27◦C, 30◦C, 33◦C, 36◦C and 39◦C), and various inlet air relative humidity (23%, 32% and 40%), the cooling performances of the proposed novel evaporative cooling system were experimentally investigated. The variations of outlet air dry bulb temperature, wet bulb effectiveness, dew point effectiveness and cooling capacity were studied by varying the incoming air dry bulb temperature. Some conclusions can be found:

1) Increase the inlet air dry bulb temperature will lead to the increase of the outlet air dry bulb temperature, cooling capacity, wet bulb effectiveness and dew point effectiveness. By keeping the inlet air dry bulb temperature at constant value, increase the inlet air relative humidity will lead to the decrease of cooling capacity, wet bulb effectiveness and dew point effectiveness;
2) The heat and mass transfer coefficients remain to be in linear relationships with respect to the Reynolds number, despite of various inlet air relative humidity. With the Reynolds number in the range of 10-220, the heat and mass transfer coefficients were in the range of 50-250W/m2K

and 0.05-0.3m/s. Two sets of non-dimensional heat and mass transfer correlations with respect to Reynolds number were deviated from the experimental results, which showed good agreements with other correlations from literature;

3) With inlet air dry bulb temperature being the same, increase the inlet air relative humidity will lead to the decrease of heat flux and mass flux. With the inlet air relative humidity being equal, increase the Reynolds number of incoming air will lead to the increase of heat flux and mass flux;

4) Experimental obtained mass transfer data are illustrated and compared with other correlations from literature. Due to the spindle shape hollow fibre module, the shielding with hollow fibre bundles could be avoided greatly, therefore the mass transfer performance of the proposed system demonstrated significant improvement compared with other devices reported in literature. The non-dimensional heat and mass transfer data comparisons indicate that the variations of experimental testing conditions have very limited impact on the heat and mass transfer correlations.

5) The wet bulb effectiveness achieved in the proposed research was between 0.3 and 0.45 with the packing fraction of 0.028. In the literature, the packing fraction was 0.28 in Zhang [21], which was about 10 times higher than what the hollow fiber module presented in this paper. However, the cooling effectiveness was only 1.5-2 times higher than that is obtained in this research. This means that the design of this hollow fiber integrated evaporative cooler prototype could provide comparably cooling performance as presented by other researchers, but with lower packing fraction factor（fewer fibers included）. The future work could be concentrated on increase the packing fraction by inserting more fibers into the one bundle, in order to potentially increase the cooling effectiveness.

## Acknowledgement

The authors would like to acknowledge the financial support and contributions from Innovate UK (project code: 131821).

## Tables

Table 1 Summary of some published research results on evaporative cooling systems

| Reference | Research method | Evaporative cooler type/materials | Inlet air temperature (◦C) | Outlet air temperature (◦C) | Wet bulb effectiveness | Conclusions |
|---|---|---|---|---|---|---|
| Wu et al. [13] | Simulation(simplified model) | Direct evaporative cooler/Porous honeycomb paper | 27-37 | 23-28 | 0.6-1.0 | 1) Frontal air velocity and pad thickness of the module are two key factors for the evaporative cooling system 2) The optimum frontal velocity was 2.5m/s |
| Lin et al. [32] | Experiment+ Simulation (ε-NTU method) | Dew point evaporative cooler/ hydrophobic material | 22-30 | 25-18 | 0.6-1.0 | 1) The saturation point of the working air is influenced by the working air ratio and channel height; 2) Overall heat transfer coefficient could achieve higher than 100W/$m^2$K |
| Zhang [33] | Experiment+ Simulation (fractal theory) | Direct evaporative cooler/hollow fiber membrane | NA | NA | NA | 1) Experimental obtained relationship between Sherwood and Reynolds number was established using fractal model; 2) Membrane module with higher packing fraction could lead to better heat transfer performance. |
| Franco et al. [14] | Simulation | Direct evaporative cooler/ Porous paper | NA | NA | 0.6-0.8 | 1)Comparisons of the cooing performance of five different porous materials revealed that the plastic grid block produced highest efficiency of 82.6%; 2) Higher efficiency will lead to lower specific water consumption |
| Zhao et al. [34] | Simulation | Dew point evaporative cooler/ Porous polygonal stack | 28◦C | NA | 0.5-1.3 | 1)Cooling effectiveness increased with the increase of the working-to-intake air ratio; 2)Under UK summer design condition, the wet-bulb and dew-point effectiveness could reach up to 1.3 and 0.9. |

Table 2 Geometric and physical properties of the polymer hollow fibre evaporative cooler

| **Property** | **Symbol** | **Values** | **Unit** |
|---|---|---|---|
| Duct cross section diameter | | 0.15 | m |
| Duct total length | L | 0.9 | m |
| Fibre number inside the module | N | 5*100=500 (5 bundles) | |
| Fibre outside diameter | $d_o$ | 0.8 | mm |
| Fibre inside diameter | $d_i$ | 0.6 | mm |
| Nominal pore size | | 0.2 | µm |
| Fibre porosity | | 0.6 | |
| Packing density | | 10.67 | $m^2/m^3$ |
| Packing fraction | $\varphi$ | 0.028 | |
| Polymer hollow fibre thermal conductivity | k | 0.17 | W/mK |

Table 3 Testing conditions of the novel polymer hollow fiber integrated evaporative cooling system

| **Property** | **Symbol** | **Values** | **Unit** |
|---|---|---|---|
| Incoming air velocity | $v_a$ | 0.1-5.0 | m/s |
| Water flow rate inside fibre | | 0.05 | l/m |
| Incoming air temperature | $T_a$ | 27-39 | °C |
| Incoming air humidity | $RH$ | 23-40 | % |

**Figures**

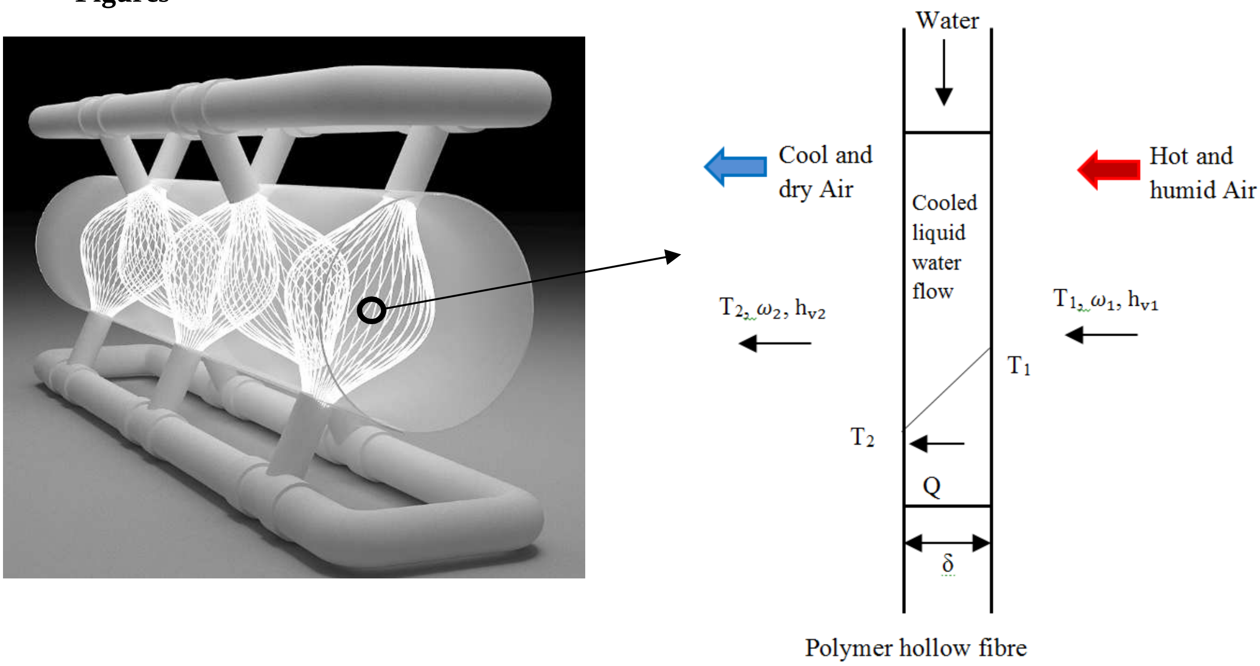


Figure 1 The 3-D model and the temperature and humidity change profile in the hollow fibre module

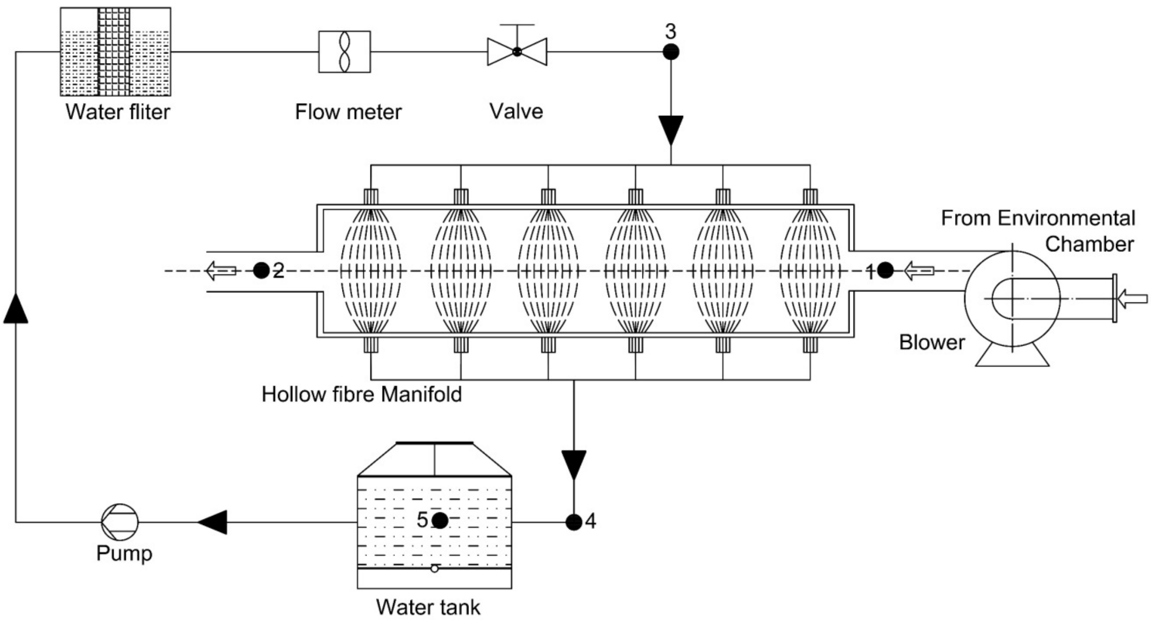


Figure 2 Schematic diagram of polymer hollow fibre integrated evaporative cooling system

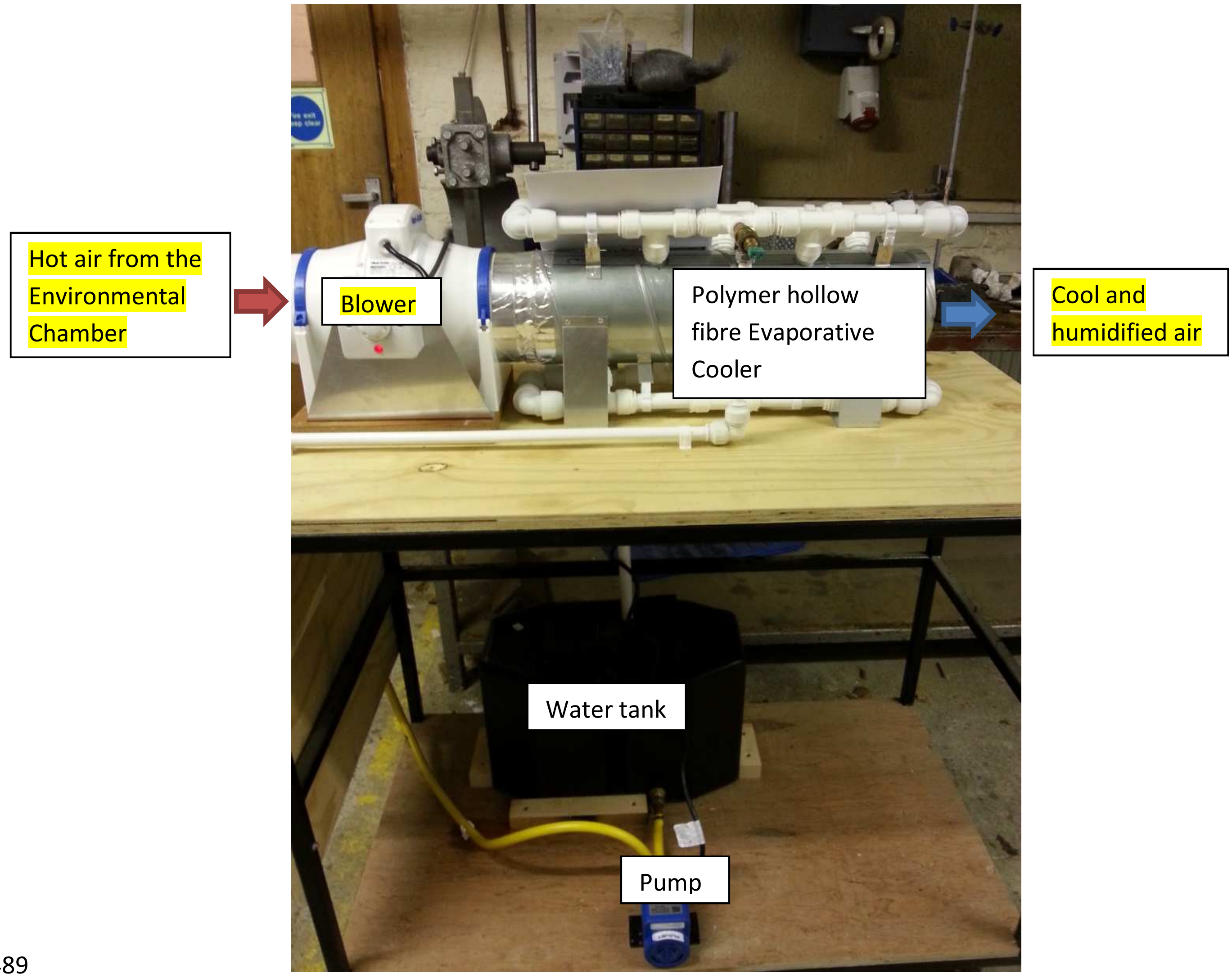


Figure 3 Testing rig of polymer hollow fibre integrated evaporative cooling system

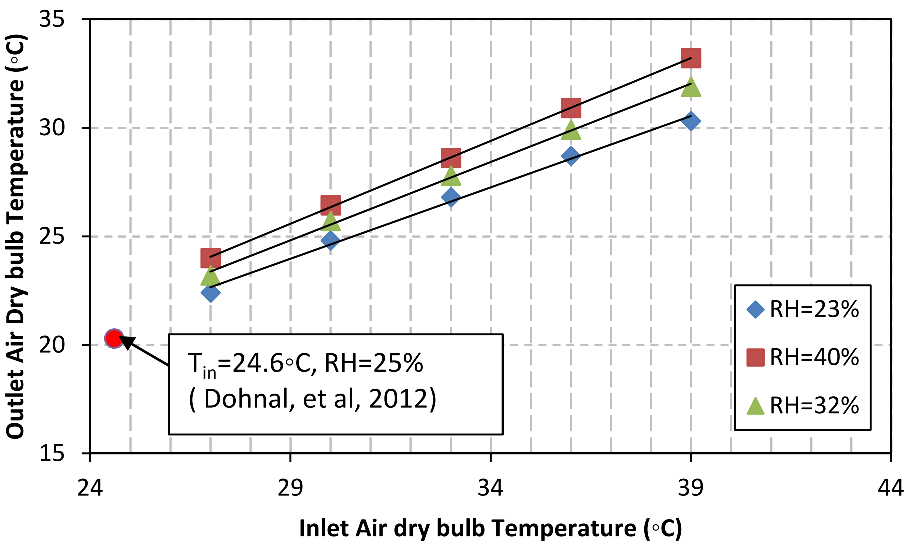

Figure 4 Variations of outlet air dry bulb temperatures with respect to various inlet air dry bulb temperatures under different incoming air relative humidity (u=4.6m/s)

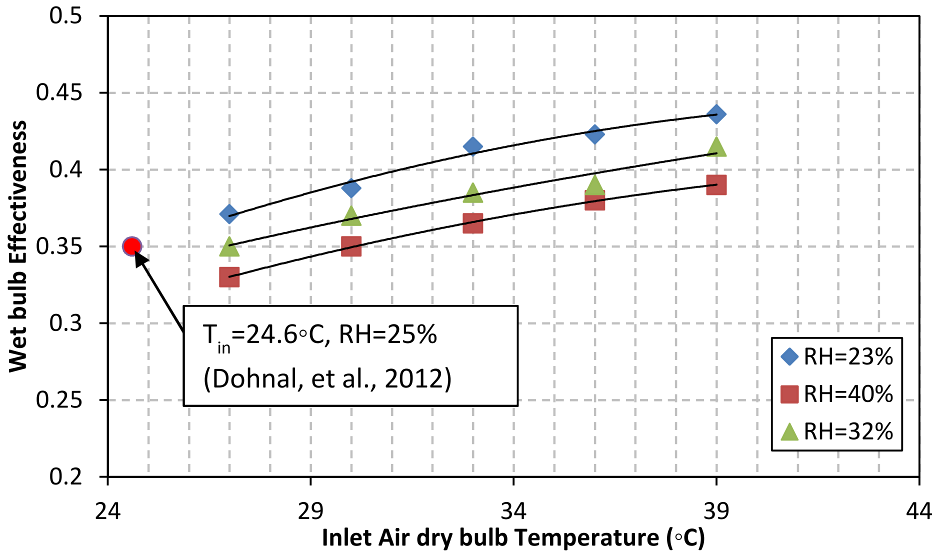


Figure 5 Variations of wet bulb effectiveness with respect to various inlet air dry bulb temperatures under different incoming air relative humidity (u=4.6m/s)

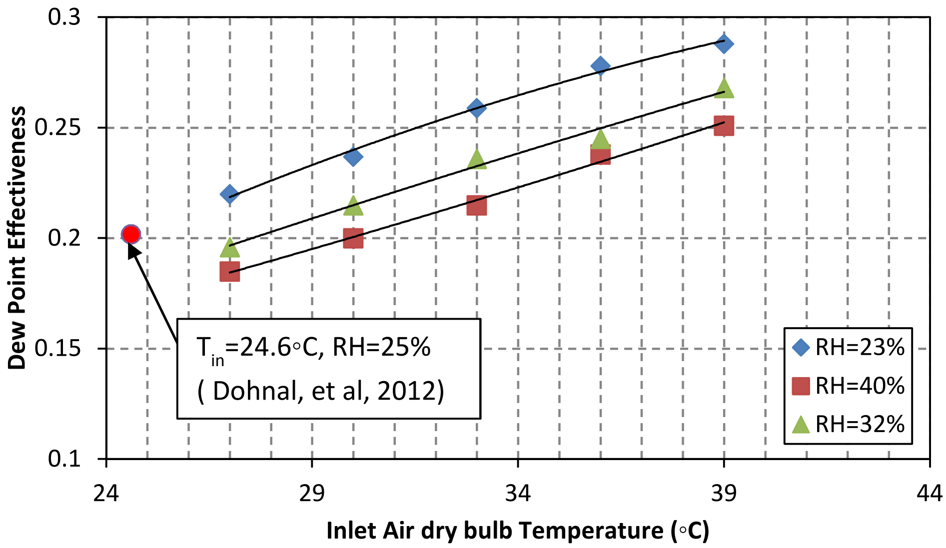


Figure 6 Variations of dew point effectiveness with respect to various inlet air dry bulb temperatures under different incoming air relative humidity (u=4.6m/s)

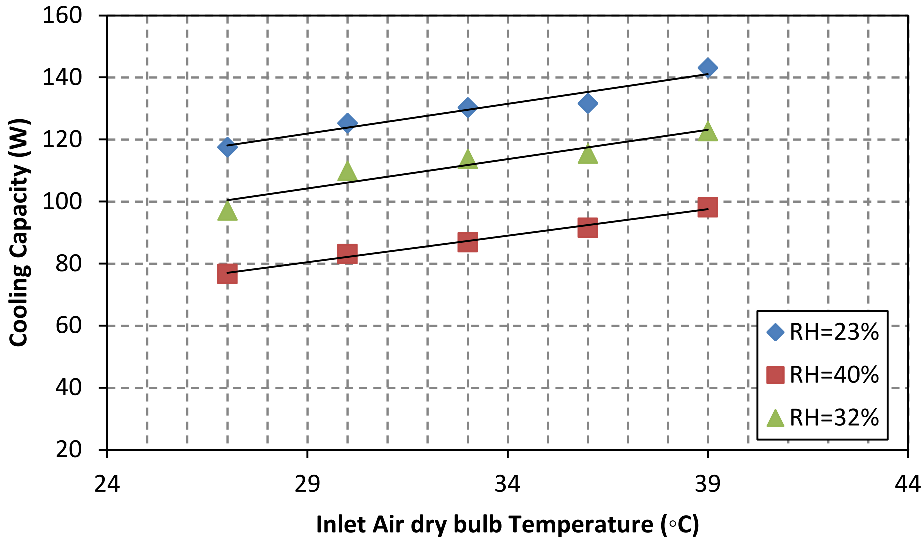


Figure 7 Variations of cooling capacity with respect to various inlet air dry bulb temperatures under different incoming air relative humidity

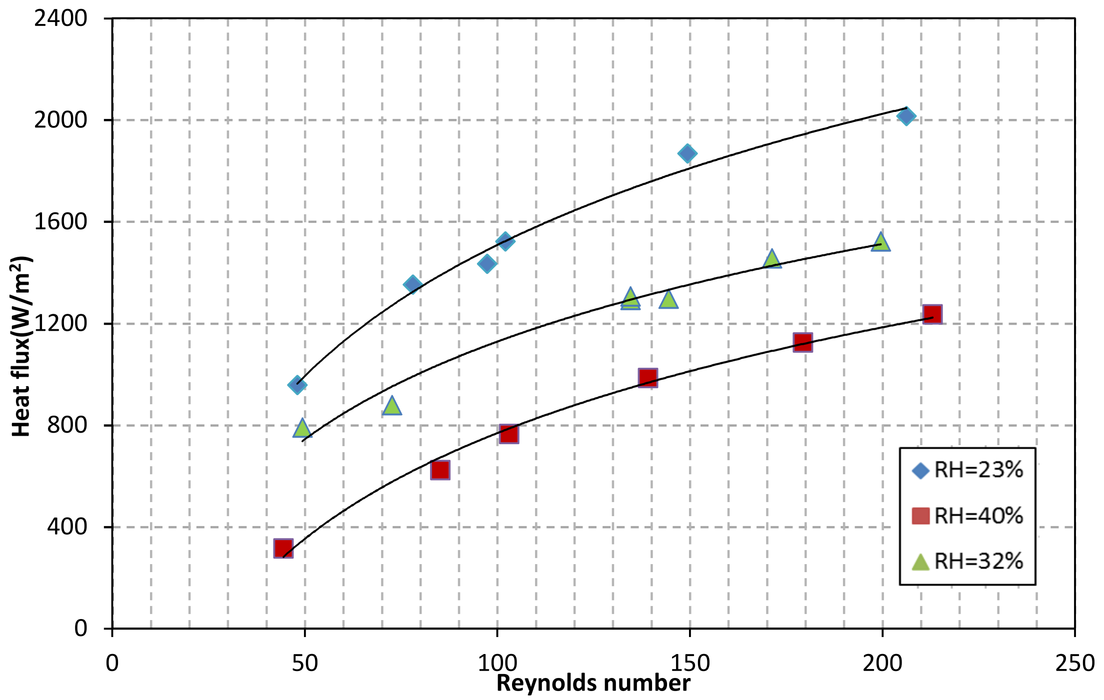


Figure 8 Variations of heat flux with respect to Reynolds number under different incoming air relative humidity

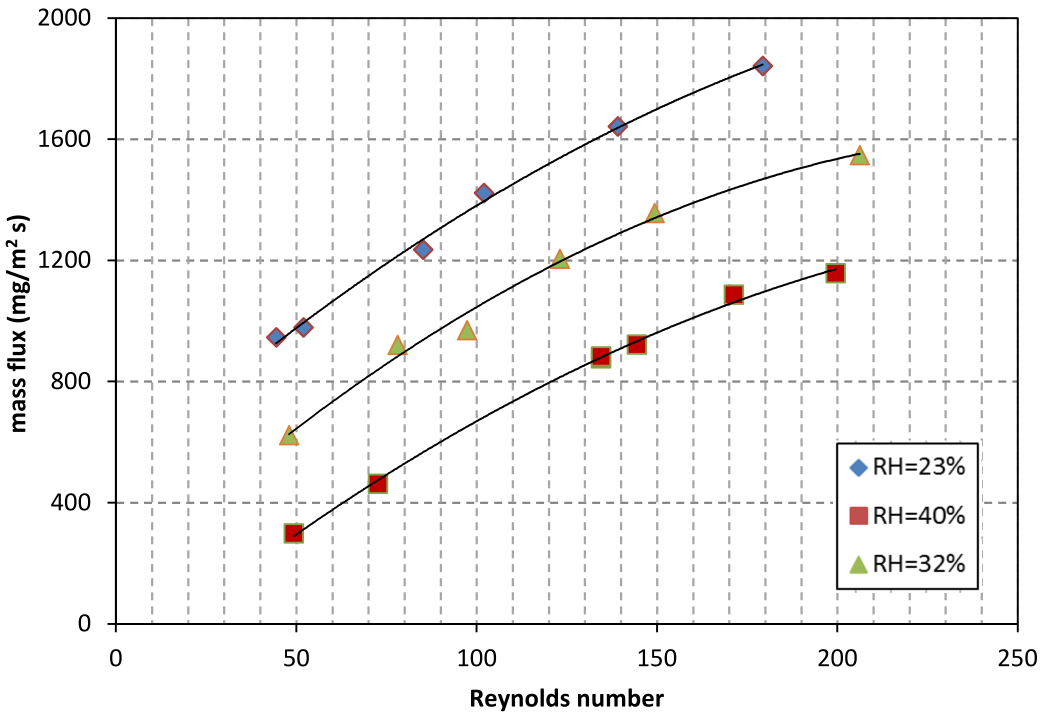


Figure 9 Variations of mass flux with respect to Reynolds number under different incoming air relative humidity

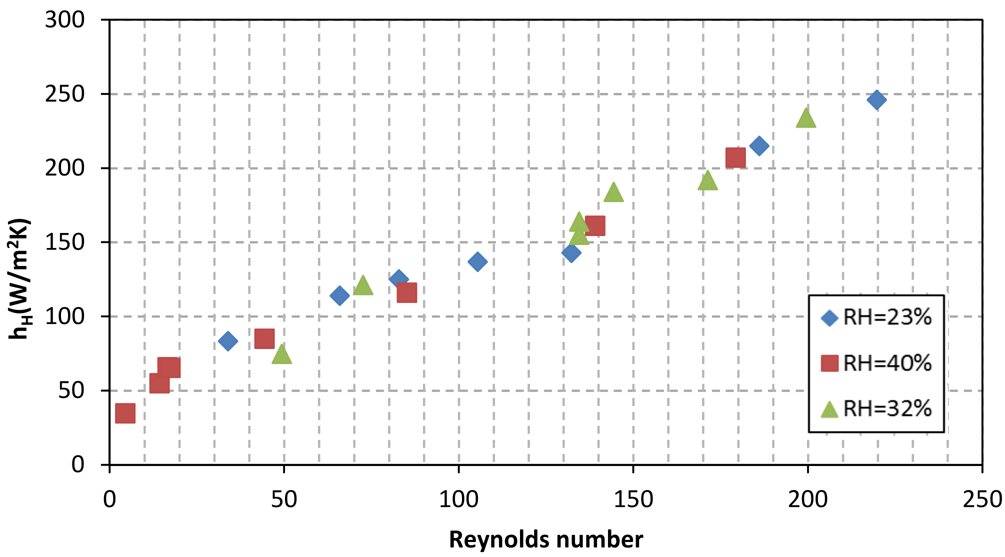


Figure 10 Variations of heat transfer coefficients with respect to Reynolds number under different incoming air relative humidity

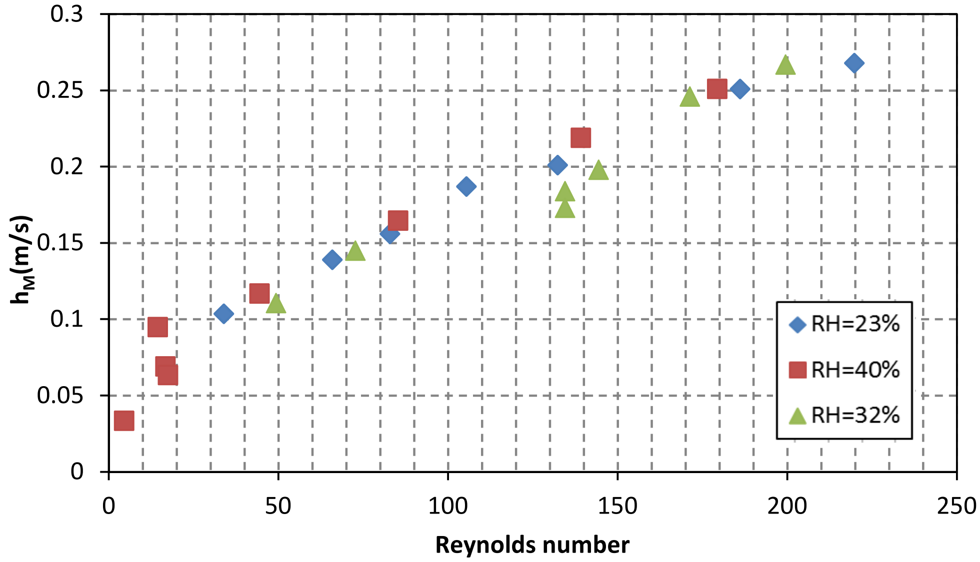


Figure 11 Variations of mass transfer coefficients with respect to Reynolds number under different incoming air relative humidity

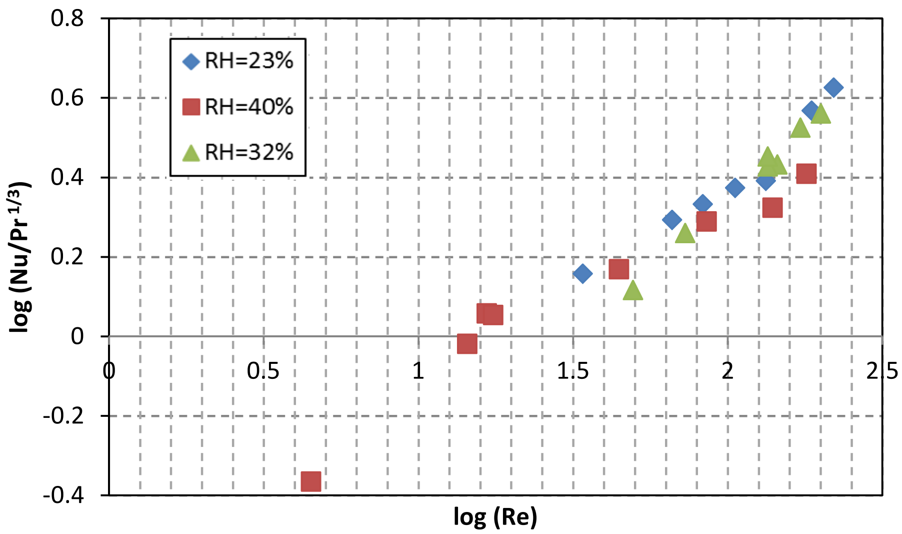


Figure 12 Variations of Non-dimensional heat transfer data under different incoming air relative humidity

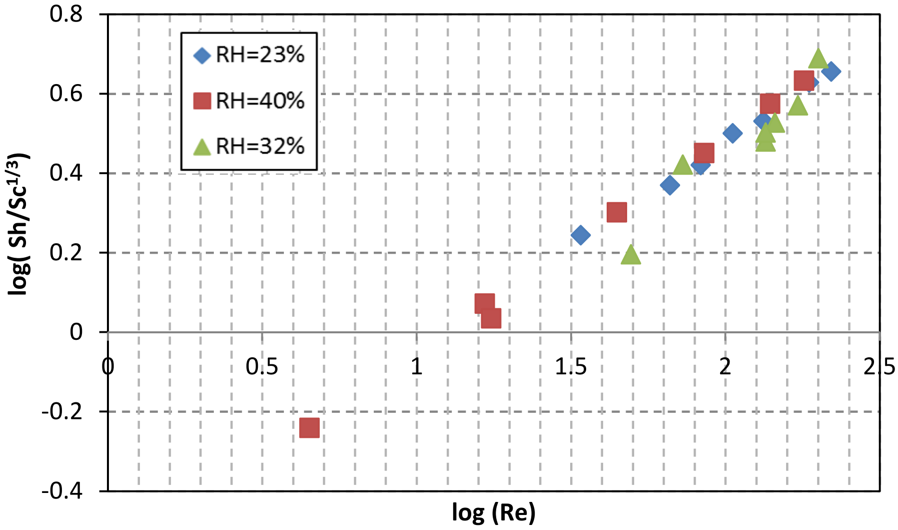


Figure 13 Variations of Non-dimensional mass transfer data under different incoming air relative humidity

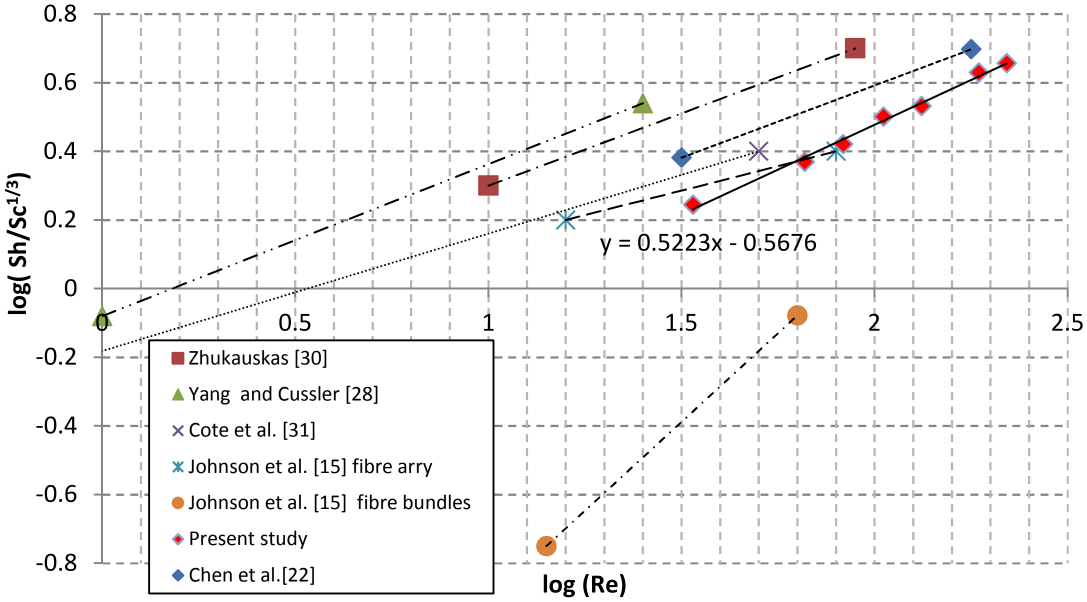


Figure 14 Comparisons of mass transfer data of presented results with other correlations in literature

## Reference

1. Choudhury, B., P.K. Chatterjee, and J.P. Sarkar, *Review paper on solar-powered air-conditioning through adsorption route.* Renewable and Sustainable Energy Reviews, 2010. **14**(8): p. 2189-2195.

2. Adnott, J., *Energy Efficiency of Room Air-conditioners (EERAC) Study, Directorate General for Energy (DGXVII) of the Commission of the European Communities.* 1999.
3. Farmahini-Farahani, M., S. Delfani, and J. Esmaeelian, *Exergy analysis of evaporative cooling to select the optimum system in diverse climates.* Energy, 2012. **40**(1): p. 250-257.
4. Liao, C.-M. and K.-H. Chiu, *Wind tunnel modeling the system performance of alternative evaporative cooling pads in Taiwan region.* Building and Environment, 2002. **37**(2): p. 177-187.
5. Rawangkul, R., et al., *Performance analysis of a new sustainable evaporative cooling pad made from coconut coir.* International Journal of Sustainable Engineering, 2008. **1**(2): p. 117-131.
6. He, S., et al., *Experimental study of film media used for evaporative pre-cooling of air.* Energy Conversion and Management, 2014. **87**: p. 874-884.
7. Mujahid Rafique, M., et al., *A review on desiccant based evaporative cooling systems.* Renewable and Sustainable Energy Reviews, 2015. **45**: p. 145-159.
8. Alahmer, A., *Thermal analysis of a direct evaporative cooling system enhancement with desiccant dehumidification for vehicular air conditioning.* Applied Thermal Engineering, 2016. **98**: p. 1273-1285.
9. Riangvilaikul, B. and S. Kumar, *An experimental study of a novel dew point evaporative cooling system.* Energy and Buildings, 2010. **42**(5): p. 637-644.
10. Caliskan, H., et al., *Thermodynamic performance assessment of a novel air cooling cycle: Maisotsenko cycle.* International Journal of Refrigeration, 2011. **34**(4): p. 980-990.
11. Zhao, X., J.M. Li, and S.B. Riffat, *Numerical study of a novel counter-flow heat and mass exchanger for dew point evaporative cooling.* Applied Thermal Engineering, 2008. **28**(14–15): p. 1942-1951.
12. Zhao, X., et al., *Feasibility study of a novel dew point air conditioning system for China building application.* Building and Environment, 2009. **44**(9): p. 1990-1999.
13. Wu, J.M., X. Huang, and H. Zhang, *Numerical investigation on the heat and mass transfer in a direct evaporative cooler.* Applied Thermal Engineering, 2009. **29**(1): p. 195-201.
14. Franco, A., et al., *Influence of water and air flow on the performance of cellulose evaporative cooling pads used in mediterranean greenhouses.* Transactions of the ASABE, 2010. **53**(2): p. 565-576.
15. Johnson, D.W., C. Yavuzturk, and J. Pruis, *Analysis of heat and mass transfer phenomena in hollow fiber membranes used for evaporative cooling.* Journal of Membrane Science, 2003. **227**(1–2): p. 159-171.
16. Chiari, A., *Air humidification with membrane contactors: experimental and theoretical results.* International journal of ambient energy, 2000. **21**(4): p. 187-195.
17. Wickramasinghe, S.R., M.J. Semmens, and E.L. Cussler, *Hollow fiber modules made with hollow fiber fabric.* Journal of Membrane Science, 1993. **84**(1): p. 1-14.
18. Chen, X., et al., *Recent research developments in polymer heat exchangers – A review.* Renewable and Sustainable Energy Reviews, 2016. **60**: p. 1367-1386.
19. Chen, X., et al., *Experimental investigations of polymer hollow fibre heat exchangers for building heat recovery application.* Energy and Buildings, 2016. **125**: p. 99-108.
20. Kachhwaha, S.S. and S. Prabhakar, *Heat and mass transfer study in a direct evaporative cooler.* Journal of Scientific & Industrial Research, 2010. **69**: p. 705-710.
21. Zhang, L.-Z., *Coupled heat and mass transfer in an application-scale cross-flow hollow fiber membrane module for air humidification.* International Journal of Heat and Mass Transfer, 2012. **55**(21–22): p. 5861-5869.
22. Chen, X., et al., *Experimental Investigations of Polymer Hollow Fibre Integrated Evaporative Cooling System with the Fibre Bundles in a Spindle Shape* Energy and Buildings, 2017. **In press**.

23. Prasad, R. and K. Sirkar, *Dispersion‐free solvent extraction with microporous hollow‐fiber modules.* AIChE journal, 1988. **34**(2): p. 177-188.
24. Zhang, L.-Z. and S.-M. Huang, *Coupled heat and mass transfer in a counter flow hollow fiber membrane module for air humidification.* International Journal of Heat and Mass Transfer, 2011. **54**(5–6): p. 1055-1063.
25. Dohnal, M., T. Vesely, and M. Raudensky. *Low cost membrane contactors based on hollow fibres*. in *EPJ Web of Conferences*. 2012. EDP Sciences.
26. Costello, M.J., et al., *The effect of shell side hydrodynamics on the performance of axial flow hollow fibre modules.* Journal of Membrane Science, 1993. **80**(1): p. 1-11.
27. Grober, H. and S. Erk, *Fundamentals of heat transfer* MCgRaw-Hill, New York, 1961: p. 233.
28. Yang, M.C. and E. Cussler, *Designing hollow‐fiber contactors.* AIChE Journal, 1986. **32**(11): p. 1910-1916.
29. Moffat, R.J., *Describing the uncertainties in experimental results.* Experimental Thermal and Fluid Science, 1988. **1**(1): p. 3-17.
30. Zukauskas, A., *Heat transfer from tubes in crossflow, in: T.F. Irvine (ed.)* Advances in Heat Transfer, Acadmisc Press, New York, 1972.
31. Cote, P., J.-L. Bersillon, and A. Huyard, *Bubble-free aeration using membranes: mass transfer analysis.* Journal of membrane science, 1989. **47**(1-2): p. 91-106.
32. Lin, J., et al., *Study on dew point evaporative cooling system with counter-flow configuration.* Energy Conversion and Management, 2016. **109**: p. 153-165.
33. Zhang, L.-Z., *Heat and mass transfer in a randomly packed hollow fiber membrane module: A fractal model approach.* International Journal of Heat and Mass Transfer, 2011. **54**(13–14): p. 2921-2931.
34. Zhan, C., et al., *Comparative study of the performance of the M-cycle counter-flow and cross-flow heat exchangers for indirect evaporative cooling – Paving the path toward sustainable cooling of buildings.* Energy, 2011. **36**(12): p. 6790-6805.

## Lists of Figures

**List of Table**